Automatic detection of defects in industrial ultrasound images using a neural network

Article *in* Proceedings of SPIE - The International Society for Optical Engineering · August 1996

DOI: 10.1117/12.248579

CITATIONS
24

READS
250

2 authors:

Shaun Lawson
Northumbria University
130 PUBLICATIONS **1,478** CITATIONS
SEE PROFILE

Graham A Parker
University of Surrey
62 PUBLICATIONS **457** CITATIONS
SEE PROFILE

Automatic detection of defects in industrial ultrasound images using a neural network

Shaun W. Lawson and Graham A. Parker

Mechatronic Systems and Robotics Research Group
Department of Mechanical Engineering
University of Surrey,
Guildford, Surrey, GU2 5XH, United Kingdom.
E-mail: s.lawson@surrey.ac.uk

ABSTRACT

Time-of-Flight Diffraction (TOFD) is a relatively new method of ultrasonic inspection and is well suited to semi-automation using methods such as robotic scanning, computer conditioned data acquisition and signal and image enhancement. However very little work has been documented on the full computer understanding of such scans. Instead, most work has been directed at aiding the manual interpretation process to determine defect characteristics.

This paper describes the application of image processing and neural networks (ANNs) to the task of completely automating the decision making process involved in the interpretation of TOFD scans. Local area analysis is used to derive a feature vector which contains two-dimensional information on defect/component and non-defect areas. These vectors are then classified using an ANN trained with the backpropagation algorithm. The labelled image is then further segmented using binary shape analysis to discriminate between component echoes, or defect signals. Time-of-Flight correction techniques may be then used in order to determine the location of defects within a scanned weld.

Keywords: non-destructive testing, defect detection, image segmentation, neural networks, ultrasonic Time of Flight Diffraction (TOFD) testing.

1. INTRODUCTION

Non-destructive testing (NDT) is used as part of the quality control cycle in many welding applications. Arguably the most commonly used method of weld NDT is ultrasonic testing (UT), which is normally undertaken with a great deal of manual interaction and interpretation. However, there remains an identifiable need for fast automatic interpretation in many applications, such as pressure vessel welding, where it is imperative that any defects that occur as a result of the manufacturing process are located immediately so as not to incur serious loss in time and expense. The inspection of large scale welded components, such as pipelines, would also benefit from an automated interpretation system.

To meet these needs, many UT systems now feature remote manipulator arms equipped with arrays of ultrasonic transducers to undertake scans of large components in a fraction of the time it would previously have taken a human inspector. However, once such a scan is completed then the operator then faces the task of the interpretation of the reflection signatures in the scan printed out by the computer. With conventional pulse echo ultrasonic testing then this interpretation is often a very complex and subjective process, made even more difficult if the component under test is of a complex geometry.

This paper describes the initial findings in work undertaken to automate the interpretation of a ultrasonic images acquired by a relatively new ultrasonic method which lends itself quite practicably to semi and even full automation -namely 'Time-of-Flight Diffraction' (TOFD) testing [1,2]. TOFD ultrasonic scans are stored in a digital form with a single 'scan' line characterising the structure of the weld at any one position. In this way, an image of the complete weld may be built, showing component and, more importantly any defect information. It is shown in

this paper that automatic interpretation of TOFD images is possible by segmenting 'interesting' signatures from background signals using texture descriptors and an artificial neural network (ANN). It is further illustrated how defect signatures can then be separated from innocuous component echoes using an intelligent splitting scheme. The attributes of any defects present can then be described (for full automatic appraisal of the weld) or their presence on the scan indicated (to aid manual interpretation).

2. ULTRASONIC TIME-OF-FLIGHT DIFFRACTION TESTING

The Time-of-Flight Diffraction (TOFD) method has only recently emerged as an accepted NDT technique for flaw detection [3] though it has been used extensively in the last fifteen years for flaw sizing [4,5] . The method relies on the diffraction of ultrasonic energies from 'corners' and 'ends' of internal structures (primarily defects) in a component under test. This is in contrast to conventional pulse echo methods which rely on directly reflected signals. The typical apparatus for TOFD weld examination is illustrated in Fig. 1. A two probe (one transmitter, one receiver) arrangement is used, with the chosen transmitter producing a relatively wide beam to maximise the extent of the scan. The two probes are aligned geometrically either side of the weld and A-scans are taken at sequential positions along the length of the weld bead. The time taken to scan a length of weld is therefore very short since no raster scanning is necessary.

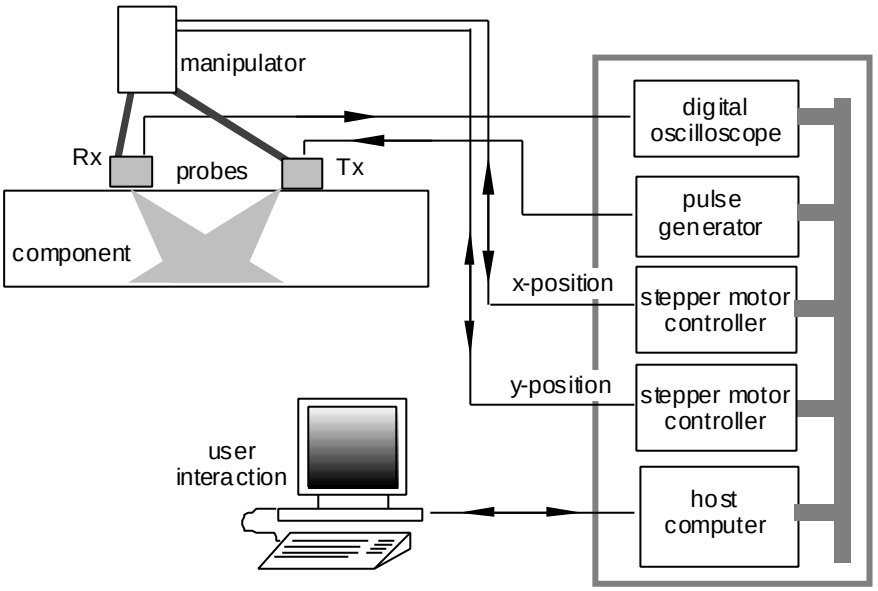

Figure (1) - data acqusisition system for ultrasonic TOFD inspection.

TOFD scans are presented as a series of non rectified RF (radio frequency) A-scan waveforms digitised directly from the receiver probe during the scanning operation. For the purpose of this work we will assume that a group of A-scans are presented as a D-scan showing the details of a weld along its length, although B-scan representations are also commonly used to assess a cross section of the weld. A typical TOFD D-scan of a steel butt weld is shown in Fig. 2a. The most obvious attribute of the scan is the backwall echo running from left to right as a wide band along the centre of the scan. Slightly less apparent is the parallel surface (or lateral) wave towards the top of the scan. These features are the two most important time measurements which may be extracted from the scan, since they give the velocity of the ultrasound through the material and also the depth and through wall thickness of any defects within the weld.

A single A-scan from the D-scan shown in Fig. 2a is presented in Fig. 2b. A human observer may recognise the RF ripple of the backwall signal with little difficulty (beginning at time t = t_b) but the lateral wave is more difficult to discern (at time t = t_1). The areas above the lateral wave and below the backwall echo can be largely ignored since they present little meaningful information. The actual period between t = 0, and t = t_l represents the probe delay, whilst signals occurring at t > t_b are due to so called 'mode converted' echoes, which are a result of physical transforms of the incident wave structure, most commonly from longitudinal to shear waves. Mode converted signals, although not of primary concern, can however be interesting since their patterns will often duplicate those to be found in the main body of the scan, i.e. the region where tl < t < tb.

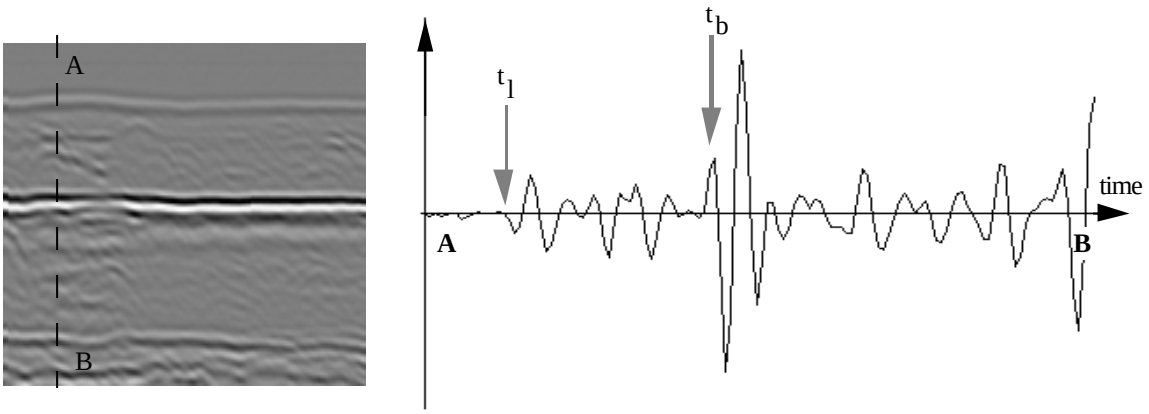

Figure (2): ultrasonic TOFD scan data. (a) 136 x 128 D-scan of butt weld in 25mm thick steel plate. (b) A-scan along line AB in (a). Note that signatures in the D-scan (backwall and surface echoes for example) are much easier to detect than in the single A-scan.

Defect echoes are characterised by ripples in the A-scan similar, though not generally so large in magnitude, to those of the backwall and lateral wave signals. These will merge together in the D-scan to form areas of grey level 'disturbance' which stand out from smaller echoes which may be due to insignificant pores, or noise spikes. There is a defect in the scan shown in Fig. 2a lying approximately half way between the surface and backwall echoes. The defect is detectable on the D-scan, but not on the A-scan. It is for this reason why TOFD data is usually presented in two dimensional images rather than in individual A-scan format - it makes for much easier detection of both the component and defect echoes.

Once a defect region is located in the D-scan the next step in the interpretation is defect location and sizing. This is achieved by first locating the backwall and surface echoes whose time of flight (TOF) may used to convert from time to depth for any point in the scan. This calculation allows accurate depth localisation of a defect and also gives an indication of its 'through wall dimension'. Defect length is more difficult to resolve because of the characteristic arcing at the ends of a defect. Several post-processing methods have been proposed to eliminate such effects and to enhance the defect signal - most notably the Synthetic Aperture Focusing Technique (SAFT) **[6]**. However, even in state-of-the-art TOFD scanning systems **[7]**, the localisation and sizing of a defect is an almost entirely manual process - an NDT operator will mark on the scan (using a mouse) where the component echoes lie, and then where a defect lies. The computer will then automatically perform the TOF correction and given an indication of the defect size according to what has been indicated by the operator. However if automatic defect detection were possible, then the TOFD testing process could be automated entirely. An automatic technique which has been developed for defect detection in TOFD images using a neural network is now described.

3. SEGMENTATION OF TOFD SCANS USING A NEURAL NETWORK

The detection of defects in a TOFD image is ideally achieved by the classification of each pixel in the image as defect or non-defect - ie. there are only two possible classes of pixel. However the local area properties of defect echoes are very similar to those of component echoes. Therefore the segmentation of TOFD images must be approached in two steps as shown in Fig. 3 - firstly the image must be segmented pixel by pixel to reveal areas of 'interest' which may be either defect or component echoes. Secondly, such segmented areas must then be classified as being of one class or the other.

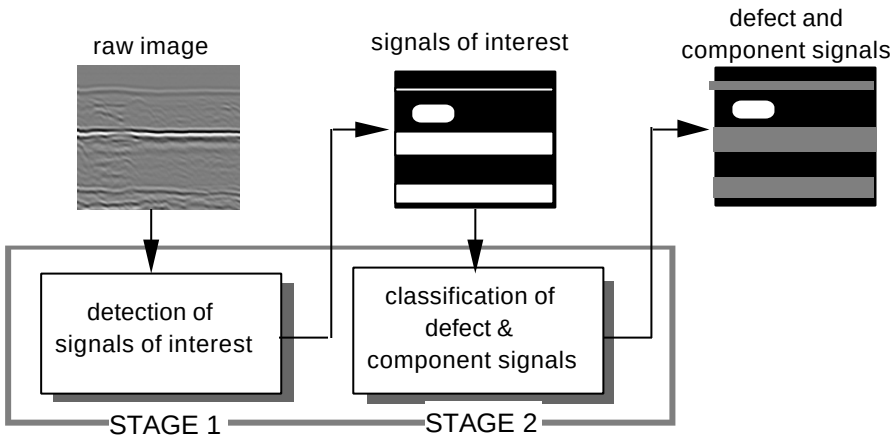

Figure (3) Two stage segmentation process for defect detection in ultrasonic TOFD images. Stage 1 labels each pixel as being of either background or object. Stage 2 then classifies blob regions as either defect or component echoes.

More specifically we are actually interested in the location of the lateral and backwall echoes and the analysis of echoes between these two signals. From such an analysis any defects may be accurately sized and located. The approach for this second stage is described in Section 4. The remainder of this section now describes a technique which performs the first stage of the segmentation using a backpropagation multi-layer perceptron (MLP) artificial neural network (ANN).

3.1 local area descriptors for TOFD image segmentation

Manual detection of defects in TOFD scans is made easier by considering the two dimensional properties of a B-scan or D-scan. In order to automatically emulate such a process, a segmentation procedure based on discriminatory analysis of the grey level population centred on the pixel to be classified has been evolved. From a local population it is a common approach to extract local features which give a higher order description of the local image content. Here we are concerned with the selection of features which will accurately segment areas of interest (objects) from background pixels in ultrasonic TOFD images. Since defects in TOFD images tend to produce sharp grey level variations between adjacent pixels then it is a reasonable assumption that a useful feature, or descriptor, to use in this case would be the variance of the local population - this is equivalent to the statistical 2nd moment, and is given by :-

$$Var = \frac{1}{N\,xN} \bullet \sum_{n=1}^{NxN} (i_n - \bar{i})^2 \qquad \text{... Equ. (1)}$$

Where (NxN) is the size of the local population and $\bar{i}$ is the mean of that population. The variance may be more conveniently represented by its square root, or the standard deviation, s :-

$$\sigma = \sqrt{\frac{1}{N\,xN} \bullet_{n=1}^{NxN} (i_n - \bar{i})^2} \qquad \text{... Equ. (2)}$$

Other descriptors which may be of value in the segmentation of TOFD images are the third and higher order statistical moments, ρ_m, given by:

$$\rho_m = \frac{1}{N\,xN} \bullet_{n=1}^{NxN} \left(\frac{i_n - \bar{i}}{\sigma} \right)^m \qquad \text{... Equ. (3)}$$

where m is the order of the moments to be calculated. The third order moments are known to give a measure of the 'skewness' of the histogram of the local population, whilst the fourth moments give a measure of histogram 'flatness' **[8]**. Such measures are perhaps more useful for discrimination between more regular textures than we are dealing with here, and have been used for example by Haralick **[9]** and many others in auto-correlation descriptions of spatial dependant pixel relationships. Also perhaps unsuitable here are frequency domain methods such as those described by Kulkarni **[10]**, because we are unable to assume regular spatial pattern repetition, and therefore mathematical modelling of our two main classes, i.e. defect or non defect, is difficult.

Despite the reliance by many researchers on higher order descriptors for local area discrimination, in some cases **[11]** it has been shown that 1st order descriptors, such as the variance (see above) and the mean, can provide comparable segmentations, and also are quicker to compute. In our case we are seeking an on-line solution to an inspection task, with the segmentation at this stage being only one step in the process - high speed of execution is therefore of extreme value. The following descriptors are all computed with little difficulty :-

- standard deviation, σ
- mean value, $\bar{i}$
- maximum value, i_{max}, in the local population,
- minimum value, i_{min}, in the local population,
- (maximum - minimum) value, $i_{max} - i_{min}$

These, and other, operators selected for their speed of extraction, have been studied by Voss **[12]** in order to determine the most useful combinations for segmentation of various synthetic and real textured images. Voss concludes that the descriptors (a), (b) (c) and (e) above, combined with the actual pixel value under scrutiny are useful features to provide discrimination between classes over a relatively small area. Max-min statistics have been described previously in the literature, for example by Mitchell et al **[13]**, for texture analysis problems. Intuitively we can deduce that to obtain an optimum segmentation it is possible to use a combination of the outputs from the descriptors used above - the problem when adopting such an approach is how to best combine the descriptor outputs. In this work a backpropagation artificial neural network (ANN) was used to achieve this.

3.2 A neural network for defect detection in TOFD images

The topology of a MLP neural network used in the work presented here is given in Fig. 4. The figure shows a three layer network incorporating a single hidden layer of processing elements (PE's). Each PE has a weighted connection to every PE in the next layer, and each performs a summation of it's inputs and passes the result

through a transfer function - this is a linear function at the input layer and a non-linear sigmoid function at every other layer.

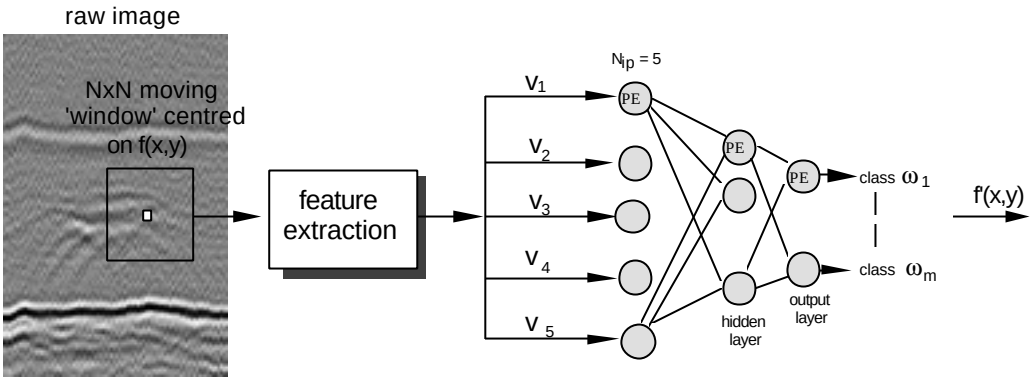

Figure (4) - ANN topology used for initial tests on segmentation of TOFD images

3.3 Training of the network

The training of MLP networks requires access to a pre-classified set of 'training data', each element of which has the form {data; class}. The majority of works which have been described in the literature which make use of supervised learning schemes for image segmentation, use training and test images of a single synthetic surface, such as textures from the Brodatz album **[14]**, or entire scenes containing the same class of pixel, or 'cut and pasted' sections of such images. In such cases it is a straightforward task to generate preclassified training data for any number of images, for example one image for each possible class of pixel. In the case dealt with here this is clearly not possible since we are concerned with images of 'real' scenes, and it is not feasible to artificially generate an entire image of 'defect' pixels and entire image of 'background pixels'.

A semi-automated segmentation method was therefore used to generate training data for this work. Training data was classified by rectifying and *manually* thresholding each normalised A-scan in a sample image, before applying binary erosion / dilation to merge fragmented areas. The images used for the training were TOFD scans of *machined testpieces* with side drilled holes representing defects. Such scans are much easier to interpret than standard scans of 'real' welds.

3.4 Optimisation of the network

A number of feed forward MLP ANNs with varying topologies were simulated in software and trained on a data file containing 1500 samples of feature vectors derived from local populations of the two training images. Of the 1500 samples, 500 were examples of definite defect, 500 of background and 500 of probable defect. Optimisation of the topology and training patterns of an ANN is a notoriously ill-defined procedure and the rules for the selection of network parameters may be described as being vague at best. Furthermore the number of variables present in the training procedure is so large as to make exhaustive comparisons of all combinations impractical. The approach adopted here was to methodically, and independently, vary what were considered the most important individual parameters of the network and to assess the subsequent network performance on the training images. The following parameters were varied :-

- Number of hidden layers (N_{hl})

- Number of hidden processing elements (N_{hpe})
- Number of training iterations (N_{ti})
- Momentum term, (a)
- Size of input population mask (NxN)

It was found that a number of different network topologies and training strategies were capable of segmenting TOFD scans. Therefore a 'minimal' network solution was adopted which, in practice, had two hidden layers each of six PE's. Two examples of scans which have been segmented by this network are given in Figs. 5 and 6. The ANN was trained to label pixels of three classes - definite echo (i.e. defect or component, or class ω_1) , probable echo (class ω_2)and definite background (class ω_3). These classes are respectively labelled white, black and grey in the segmented images.

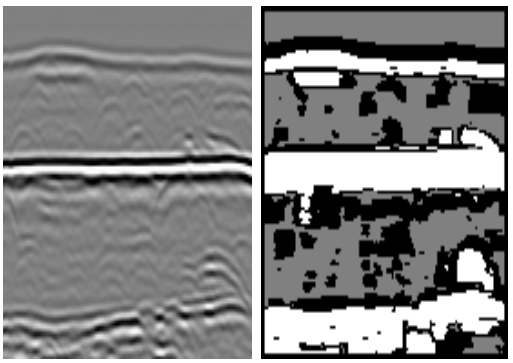

(a) (b)

Figure (5) - segmentation of example TOFD D-scan of TIG weld in 25mm steel plate. Two defects are present - one near to the top left of the scan (just below the lateral wave), and a second near the bottom right - just above the backwall echo.(a) raw scan (dimensions 136 x 128). (b) ANN segmentation.

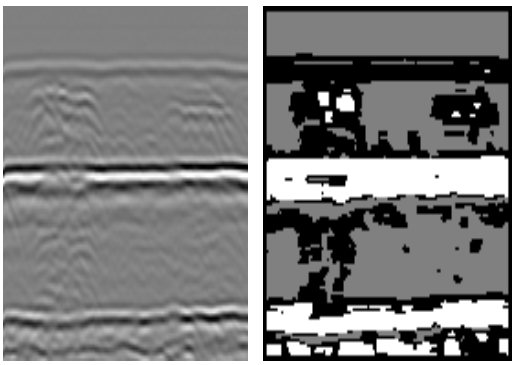

(a) (b)

Figure (6) - segmentation of example TOFD D-scan of TIG weld in 25mm steel plate. Two defects are present - both towards mid depth of the scan. The left hand defect is much more extensive than the other, which may in fact be a minor slag inclusion. (a) raw scan (dimensions 136 x 128). (c) ANN segmentation.

It can be seen in both the examples given that the ANN detects the backwall echo and in Fig. 5 also the lateral (surface) wave. It also detects both defects in Fig. 5 - although the bottom right hand defect is merged with the backwall signal - this problem is addressed in section 4. In Fig. 6 although the defects and lateral wave are not labelled of maximum interest (i.e. white) they are clearly segmented from the background (grey) and labelled as being of potential interest (i.e. labelled black). It is here where the usefulness of employing three pixel classes is seen - if more sensitivity is required with a particular scan then the areas of potential interest may be analysed in addition to areas of high interest. In both example scans, pixel areas are smoothly segmented with very few fragmented areas or sudden changes in pixel class over local regions.

4. FULL AUTOMATIC INTERPRETATION OF THE SEGEMENTED SCAN

As was explained in section 3, it is necessary to post process the segmented TOFD images in order to distinguish between defect and component echoes. In addition the time-of-flight (TOF) of any flaws which are present must be converted to actual depth measurements which may be used to assess both the severity of a flaw and the action, if any, required to rectify it.

4.1 Analysis of binary regions

Once an image has been segmented it is necessary to produce an objective description of each region, or object, so that a classification of each object can be made - most importantly whether the object is a defect or a component echo. Firstly however, each object region must be defined and described. The method chosen to do this was the blob colouring technique described by Ballard and Brown **[16]**. Following this, each separate coloured object or 'blob' in such an image may then be analysed to give a number of simple geometric measurements. The following descriptors, of each of the R regions in an image, were chosen to characterise each region :-

- region pixel area (Area),
- centre co-ordinates (C_{xr}, C_{yr}),
- maximum and minimum extremum x co-ordinates, $xmax_r$, $xmin_r$
- maximum and minimum extremum y co-ordinates, $ymax_r$, $ymin_r$
- simple horizontal length (L_r),
- simple vertical height (H_r),

These descriptors were used as the basis of classifying the objects as to being either defect or component echoes as described in the next subsection.

4.2 Location of lateral wave and backwall echoes

Once regions have been analysed it possible to address the problem of locating the main component echoes in the scan - i.e. the backwall and lateral (surface) wave signals. On D-scans, which are the main type of scan dealt with here, both of these signals should be present as horizontal regions traversing the entire width of the scan. A TOFD scan is usually acquired so that the backwall signal occurs roughly halfway along the individual A-scan. The lateral wave is usually centred very near to the top of the scan. Also present, towards the bottom of the scan, will be a mass of mode converted backwall echoes. However, for the purpose of this analysis we shall ignore mode converted signals ie. anything which falls below $t = t_b$. Hence we are interested in the location of $t = t_l$ and $t = t_b$.

The procedure adopted to automatically detect the backwall echo was to locate the object with a horizontal width the same as that of the entire scan which was also located y-centrally in the image, i.e. $C_{xr} \tilde{} (t_{max}/2)$ and $L_r \tilde{}$ total number of A-scans. The automatic location of the lateral wave was more problematical - especially since it may not always be labelled as ω_1 by an ANN segmentation. The solution adopted was to locate the first object in the image of width approaching that of the entire width of the scan. If no such object was found at a shorter time, t, than t_b, then ω_2 objects were also analysed. This procedure was found to be successful with all available scans.

(a) (b)

Figure (7) - (a) initial automatic estimation of component signals and defects in segmented image shown in Fig. (5) (b) result after splitting of any defects which have been merged with component signals.

The location of the component echoes in the segmented scan shown in Fig. 5 are shown in Fig. 7a labelled as grey whilst defect signals are retained as white - note that the defect near to the backwall echo is actually merged to

that region and as such is incorrectly deleted as a defect. This is clearly non-desirable since a defect near to either the root or the surface of the weld may have particular bearing on the quality the weld. Therefore, techniques were devised for the 'splitting' of potential defects from both the lateral wave and backwall echoes. The two problems require two separate approaches - (1) analysis of the lower edge of the lateral wave, and (2) analysis of the upper edge of the backwall signal.

If no defects have been merged with the backwall region (i.e. the backwall is 'normal') then its upper edge will be relatively smooth, parallel with the scan and show little deviation from its path. If however, a defect has merged with the backwall then this will result in a grouped cluster of significant deviations from the modal backwall edge. The procedure adopted was to determine both the local one-dimensional gradient along the upper edge of the backwall and also the local deviation from the edge mode vale. If either of these parameters, calculated for each A-scan, were found to exceed accepted small threshold values, then any such A-scan was deemed to contain merged defects which were then split from the backwall at the mode value of its upper edge. Any isolated split 'defects', due to noise for example, present in only one or two A-scans were then removed by post processing.

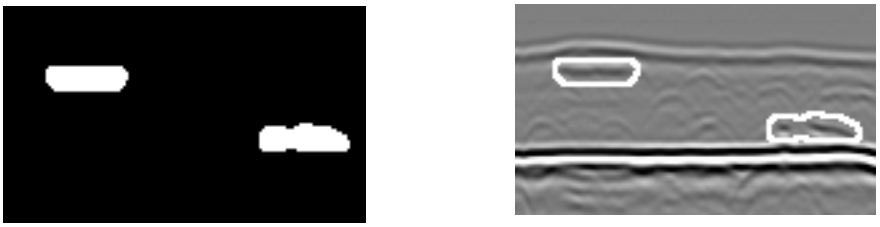

(a) (b)

Figure 8 - (a) defect merging on image shown in Fig. 7b. (b) final result of defect detection procedure overlaid on original scan.

This procedure is shown, applied to the TOFD scan in Fig. 7a, in Fig. 7b. A similar procedure was also be adopted to split defects from the lower edge of the lateral wave. Once any defects are split from region due to component signals then the modal upper edge values of the lateral and backwall wave regions give the values for t_l and t_b respectively.

4.3 Defect analysis and time of flight correction

Once the backwall and lateral waves have been confidently located and any merged defects split from these regions, then a full description of any defects which are present can be extracted. The first stage in this procedure is to merge any defect areas which have become fragmented due to the segmentation procedure. The method used to merge defect areas was a sequence of binary erode and dilate morphological operations. The application of two binary merging steps on the remaining defect blobs in Fig. 7b is given in Fig. 8a. It can be seen that the fragmented second defect (near the backwall) has been correctly merged to form a single region. Edge detections of remaining defect regions may then be overlaid on the original scan to aid manual interpretation of the inspection results, as in Fig. 8b.

Following defect merging, a second blob colouring and analysis operation is then applied so a full description of each *merged* defect region may be extracted. A time of flight correction (TOF) procedure **[2]** may then applied to all defect depth measurements extracted from the scan - i.e. C_{ry}, $ymax_r$ and $ymin_r$. The extremum depth measurements of a defect serve not only to locate its position in the weld (essential if the defect requires grinding out) but also to give an indication of its size and therefore its severity - in particular the through wall depth measurement (given by ($ymax_r$ - $ymin_r$)) is of concern in most NDT procedures. TOF to depth corrections make use of the located backwall, t_b, and lateral wave, t_l, times as starting points to derive the velocity of the sound wave

through the material. Also required are the thickness of the material, T, the probe separation, S, and sampling frequency f_S which are recorded during the scanning operation.

5. SUMMARY

Techniques for the automatic detection and characterisation of defects in TOFD ultrasonic scans have been described. The segmentation method makes use of a number of local two dimensional image descriptors which are grouped in a feature vector. A classification of the centre pixel of the local region is then obtained using an artificial neural network (ANN) to classify the vector.

The segmentation of TOFD scans must be post processed so that component and defect echoes are classified. Binary shape analysis and simple rule based reasoning are used to locate component (backwall and surface waves) signals, and also to 'split' any defects which may have been merged with these areas during the segmentation. Defect areas may then be analysed further, using time of flight correction, to give actual positional and size information. It is considered that these statistics may then be used to automatically generate a quality appraisal of a scanned weld.

6. ACKNOWLEDGEMENTS

The authors wish to acknowledge the funding of this work by the Commission of the European Communities under the Brite-EuRam II (Industrial & Materials Technologies) shared cost project scheme (project number: 5907). In particular the authors wish to thank one of the partners of this project, Mitsui Babcock Energy Ltd, for providing image data and interpretation skills.

7. REFERENCES

1. Silk, M.G., "Sizing crack like defects by ultrasonic means", in **Research Techniques in Non-destructive Testing**, vol. 3, ed. by R.S. Sharpe, Academic Press, London, 1977.

2. Carter, P., "Experience with the time-of-flight diffraction technique and an accompanying portable and versatile ultrasonic digital recording system", **Brit. J. of NDT**, Sept. 1984, pp 354-361.

3. Verkooijen, J., "TOFD used to replace radiography", **INSIGHT**, vol. 37(6), pp. 433-435, June 1995.

4. Silk, M.G., "The use of diffraction based time-of-flight measurements to locate and size defects", **Brit. J. NDT**, vol. 26, 1984, pp 208-213.

5. Silk, M.G., "Changes in ultrasonic defect location and sizing", **NDT International**, vol. 20(1), 1987, pp 9-14.

6. Seydel, J., "Ultrasonic synthetic-aperture focusing techniques in NDT", in **Research Techniques in Nondestructive Testing**, vol. (6), pp. 1-47, ed. by R.S. Sharpe, Academic Press, London, 1982.

7. Silk, M.G., "Benefits of signal processing in ultrasonic inspection", **INSIGHT**, vol. 36(10), 1994, pp 776-781.

7. Silk, M.G., "The rapid analysis of TOFD data incorporating the provisions of standards", in **Proc. of 6th European Conf on NDT**, 1994, pp 25-29.

8. Gonzalez, R.C. and Woods, R.E., **Digital Image Processing**, Addison Wesley, 1992.

9. Haralick, R. M., Shanmugam, R., and Dienstein, I., "Textural features for image classification", **IEEE Trans on Systems, Man, and Cybernetics**, vol. 3 (6), 1973.

10. Kulkarni, A.D., **Artificial neural networks for image understanding**", Van Nostrand Reinhold, New York, 1994.

11. Weszka, J.S., Dyer, C.R., and Rosenfeld, A., "A comparative study of texture measures for terrain classification", **IEEE Trans on Man, Systems and Cybernetics**, vol. SMC-6, no. 4, pp. 269-285, 1976.

12. Voss, T., "To investigate the use of artificial neural networks for texture processing in automated inspection", **Final Year Project Report No. 68, Dept. of Mechanical Engineering, University of Surrey**, 1995.

13. Mitchell, O.R., Myers, C.R. and Boyne, W., "A max-min measure for image texture analysis", **IEEE Trans on Computers**, pp. 408-414, 1977.

14. Brodatz, P., **Textures: a photographic album for artists and designers**, Dover Publications, 1966.

15. Ballard, D.H., and Brown C.M., **Computer Vision**, Prentice-Hall, 1982.